ON THE SUPERCRITICAL FLUID UNDER THE BRITTLE-DUCTILE BOUNDARY IMAGED BY MAGNETOTELLURIC STUDIES IN NE JAPAN

Yasuo Ogawa[1], Masahiro Ichiki[2]

[1]Volcanic Fluid Research Center, Tokyo Institute of Technology, Tokyo, Japan

[2]Graduate School of Science, Tohoku University, Sendai, Japan,

oga@ksvo.titech.ac.jp

Keywords: *Brittle-ductile transition, Super critical fluids, resistivity, magnetotelluric modeling*

ABSTRACT

Supercritical fluid is a new geothermal resource. We have been conducting multiple wide-band magnetotelluric surveys in NE Japan including geothermal areas. We have found mid-crustal conductors which become shallower towards the known geothermal fields around Naruko-Onikobe-Kurikoma area, based on the three-dimensional modeling of resistivity structures. The top of the conductor is consistent with the cutoff depth of the crustal seismicity. Thus the conductor is located just below the brittle-ductile transition zone. The conductor is interpreted as a high salinity fluid bearing zone. The seismicity over the conductors suggests that the migration of the fluids into the brittle zone through the brittle-ductile boundary may induce seismicity by increasing the pore pressure in the brittle zone. The conductor below the brittle zone implies the existence of super critical fluids, and possible permeability, below the brittle-ductile boundary.

1. INTRODUCTION

Super critical fluid, which underlies conventional geothermal resources (Asanuma et al., 2012; Dobson et al., 2017), is a new target for geothermal energy. In order to image such deep geothermal resources, the magnetotelluric (MT) method, which utilizes the natural electromagnetic field, is one of the best methods for deep exploration (Frioleifsson et al,. 2014; Gasperikova et al., 2015).

The MT method involves the measurement of time-varying natural electromagnetic fields and enables the remote detection of small volumes of fluid or melt in the crust and upper mantle (e.g., Wannamaker et al. 2009; Ingham et al., 2009; Bertrand et al., 2012; Hill et al. 2015). The bulk resistivity of the fluid- or melt-bearing rock is not controlled by the resistivity of the host rock, which is normally as resistive as 10^6 Ωm, but by the interconnectivity of the conductive fluid or melt in pore spaces or along grain boundaries, which can reduce the host resistivity to below 1 Ωm. Thus, the sensitivity of the electromagnetic method allows the detection of minor amounts of fluid, and the interconnectivity of fluids or melts in the crust and mantle. The transport of these minor amounts of fluid through the rock can also be estimated since the required connectivity must fit the low bulk resistivity of the rock.

Fluids play an important role in subduction systems (e.g., Iwamori, 1998). Northeastern (NE) Japan can be classified as a typical subduction zone and is therefore a suitable test site for the study of fluid distribution. The dehydration of the subducting slab in the mantle wedge results in the upwards migration of fluids, causing peridotite to be converted to serpentine, which may be detected as conductive anomalies. Fluids can also lower the melting point of peridotite and magmatic melts, a process that occurs as fluids are created and transported upwards towards the crust (Kawamoto et al., 2012; Ichiki et al., 2015). The previous 2D MT studies also found the presence of fluids in the crust which cause localized deformation and seismicity (Ogawa et al., 2001; Mitsuhata et al., 2001; Hasegawa et al., 2005; Ogawa and Honkura, 2004; Wannamaker et al., 2009). These studies showed that zones of high seismic activity were associated with resistive zones underlain by mid-crustal conductors. The observations are consistent with a fault-valve model (Sibson et al. 1988, 2009; Weatherley et al., 2013).

Since 2010, we have been conducting detailed, fine-grid MT surveys using wideband and long period MT equipment for 3D imaging of fluids in the crust and upper mantle (Ogawa et al., 2014; Ichiki et al., 2015). In this paper, we will review some results on the three-dimensional imaging of the distribution of super-critical fluid below the geothermal zones.

2. MAGNETOTELLURIC OBSERVATIONS

2.1 Magnetotelluric imaging of the subduction system

Long-period magnetotelluric observations were carried out in NE Japan from 2010 to 2013 to investigate the three-dimensional resistivity distribution of the subduction system (Fig. 1). Incorporating prior information about the subducting slab into the inversion scheme, we obtained a three-dimensional resistivity model using the code of Siripunvaraporn and Egbert (2009). The final model is characterized by a vertical conductive zone from the subducting slab surface to the lower crust beneath the Ou Backbone Range (Fig.1). The conductive body indicates a saline fluid and/or melt pathway originating from the subducting slab surface to the lower crust. The lower crust conductor is less than 10Ωm, and we estimate a saline fluid and/or melt fraction of at least 0.7vol.%. One of the across-arc cross-sections revealed that the conductive body segregates from the subducting slab surface at 80–100km depth and takes an overturned form toward the back arc. The head of the conducting body reaches the lower crust just beneath Mt. Gassan, one of the major rear-arc volcanoes in the system.

This study showed the pathway for deep slab fluids to the active volcanic arc. The more detailed fluid distribution around the volcanoes has been studies by wideband magnetotelluric soundings with close spaced grids, as shown later.

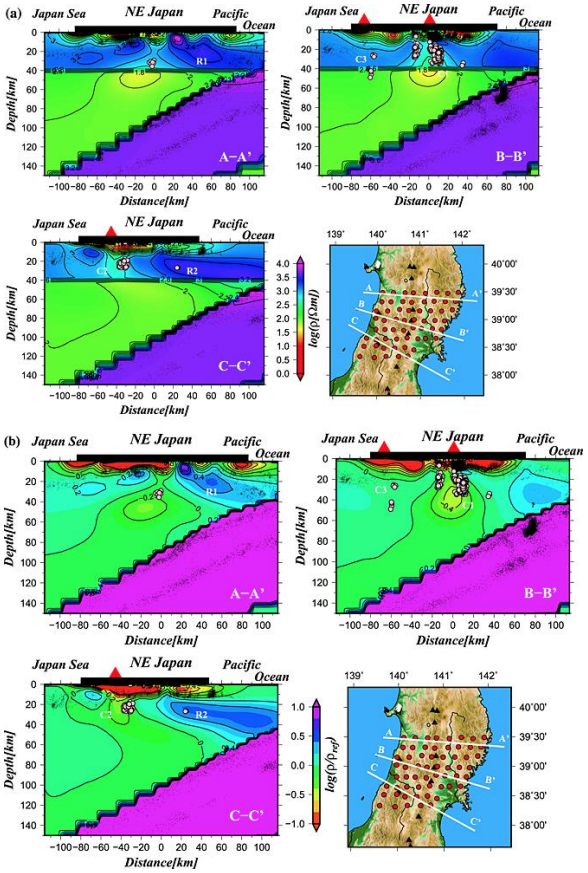

Figure 1: 3D model results from long-period MT soundings. (a) Across-arc resistivity cross-sections. Black dots and pink circles in the resistivity profile represent normal micro earthquakes and low-frequency tremors. Red triangles and thick horizontal solid lines show volcanoes and land area. C1 to C3 and R1 to R2 are major conductors and resistors. (b) Same as Figure 1(a) in terms of the resistivity perturbation from the reference mode (See Ichiki et al. (2014) for more details).

2.2 Magnetotelluric imaging of the geothermal system around Naruko volcano

The 3-D distribution of fluids was investigated using wideband MT data around Naruko volcano, NE Japan (Fig.2), which corresponds to the area in the center of the B-B' profile in Figure. 1. Full-component impedance tensors at eight representative periods at 77 sites were used in the inversion, using a 100-Ωm uniform earth with surrounding ocean as the initial model.

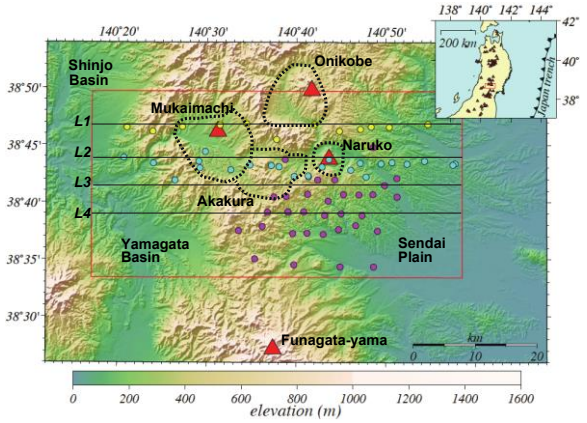

Figure 2: Magnetotelluric sites around Naruko volcano. Major Quaternary volcanoes are shown by triangles. Late Miocene collapse calderas are outlined.

Figure 3 shows depth sections. Each panel also shows the seismic hypocentral locations with a depth tolerance of 2 km from the 1997–2011 seismic catalogue compiled by the Japan Meteorological Agency. At depths of 1 and 3 km (Figure 3a and 3b), electrical conductors C1 and C2 are located at Naruko and Mukaimachi volcanoes, respectively and represent caldera fill. Conductors C3 and C4 represent sedimentary layers of the Shinjo and Yamagata basins, respectively (Figure 2).

Structures at 5 km depth (Figure 3c) show more resistive features in general. At a depth of 10 km (Figure 3d), a conductor on a 10km scale appears to the west of Naruko volcano. The seismicity at these depths is located in the resistive region, in particular R2, which lies between conductors C1 and C2.

Deeper structures (Figure 3e–3h) show elongation of conductor C1 along the NNE–SSW direction (which is consistent with the strike of the arc), and clearer contrast with the eastern resistive block R2. The eastern conductor C2 disappears at depths below 25 km.

Long-period earthquakes at 20–30 km depth are shown in Figure 3f–3h in white dots, and presumably imply injections of magmatic melt into the crust, although their locations are distant from conductor C1 and Naruko volcano (~10 km away). The long-period earthquakes are located at the edge of the resistive block R2 and are not associated with a significant conductive anomaly.

Resistivity sections for L1 to L4 in Figure 2 are shown in Figure 4. We observe clusters of earthquakes above conductor C1. The brittle–ductile transition is defined by the cutoff where the seismicity coincides with the top of conductor C1. Thus, we interpreted C1 not as a melt, but as a saline fluid reservoir. The conductive feature extends smoothly to the west; however, there is a sharp resistivity contrast between C1 and resistor R2 in the east. Farther to the east of resistor R2, there are clusters of long-period volcanic earthquakes (shown as white dots) in the lower crust.

Section L2 shows that the leading edge of C1 conductor is shallow and approaches the surface conductor C2, which is in the middle of Naruko caldera. The level of shallow

seismicity is high along the profile, and the hypocenters are distributed in the resistive body surrounding the conductor C1. The C1 conductor implies a pathway of saline fluid at depth extending to the surface. A helium-isotope anomaly provides direct support for such a supply from the upper mantle to the Naruko volcano (Asamori et al. 2010; Horiguchi et al. 2010). Similar vertical conductors were also observed below Onikobe caldera (Fukino 2011), to the north of the study area.

Section L3 (Figure 3c), oriented east–west and located 5 km south of Naruko volcano, shows that the top of the sub-vertical conductor (C1) is deeper and its resistivity is higher than in L2 (Figure 3b). We also observed deeper hypocenters above the C1 conductor. Section L4, located 5 km farther south, is characterized by a more blurred and deeper C1 conductor. Correspondingly, the hypocenters are also deeper, being close to 15 km depth.

The mid- to lower-crustal conductors in this study showed resistivities of 1–10 Ωm. As shown in Figures 4, the top of the sub-vertical conductor is directly below the hypocenters, i.e., just below brittle-ductile transition. The existence of the conductor could imply the presence of saline fluids rather than magmatic melt, although these are not easily discriminated purely on resistivity value alone. If we assume a fluid salinity we can infer the minimum porosity, based on a fluid-bearing rock model such as Hashin–Strikman bounds (Hashin and Strikman 1962; Pommier and Le-Trong 2011). According to Nesbitt (1993), typical crustal fluids have resistivities of 0.01–1 Ωm. Recent mantle xenolith studies by Kawamoto et al. (2013) reported the salinity of fluids in the mantle wedge to be 5.1 wt%, which is more conductive than that of seawater, but the difference is a factor of <10. Here we made a first-order assumption that the fluid conductivity is 0.1 Ωm, which corresponds to a salinity four times as high as that of seawater. The Hashin–Strikman bounds for the fully connected fluid case require a porosity of 1.5%–15% for a conductive anomaly of 1–10 Ωm (Pommier and Le-Trong 2011). Shimojuku et al (2014) also showed that fluid of high salinity (>10wt%) is required to account for 10 Ωm bulk resistivity, from the resistivity measurement of fluid-bearing rocks under lower crustal conditions.

We can compare the resistivity sections with the seismic tomography results presented in Okada et al. (2014). The sub-vertical conductor C1 below Naruko volcano corresponds to both Vp and Vs images that show low velocity anomalies (approximately 5%) from the lower crust to the surface. However, the lower part (>15 km depth) shows high Vp/Vs (>1.82), whereas the upper part (<15 km) shows low Vp/Vs (approximately <1.75). The lower part, which shows low Vp, Vs but high Vp/Vs, is interpreted as representing a partial melt. The upper part, which shows low Vp, Vs but low Vp/Vs, is interpreted as a zone of high fluid content (Okada et al. 2014). The lower solubility of quartz in the upper crust (Saishu et al. 2014) will create a sealing cap for the deeper fluid due to precipitated quartz. The reduced solubility of quartz in the upper crust may also contribute to the lower Vp/Vs ratio (Christensen 1996). Thus, our electrical image, as well as the seismic image, is consistent with quartz-solubility controls on the distribution of saline fluid in the crust.

2. Conclusion

We have imaged distributions and fluid pathways from the subducting plate to the crust under the NE Japan arc, in particular near the Naruko volcano.

The crustal model shows a sub-vertical conductor, C1, below Naruko volcano. The conductor shows a sharp contrast at the eastern border of the volcanic front, compared with a blurred western border. The depth to the conductor is shallow in the vicinity of Naruko volcano and increases towards the north and south. At a depth of ≥15 km, the conductor is elongated NNE-SSW. The crustal seismicity distribution shows a cut-off depth consistent with the top of the conductor at depth. Near Naruko volcano, levels of shallow seismicity (<5 km) are high and are associated with the top of the sub-vertical conductor, which is close to the surface. This observation suggests that the crustal seismicity is fluid driven. The fluids are presumably supplied by a partial melting zone at greater depth, and the top of the fluid reservoir is capped by a self-sealed precipitation of silicate solution at temperatures of around 400°C.

Distribution of fluids, imaged as a electrical conductor, implies the existence of porosity and permeability below the brittle ductile transition, as shown by Watanabe et al. (2017).

ACKNOWLEDGEMENTS

This study was supported by JSPS KAKENHI Grant Number 21109003.

(a) 1km depth

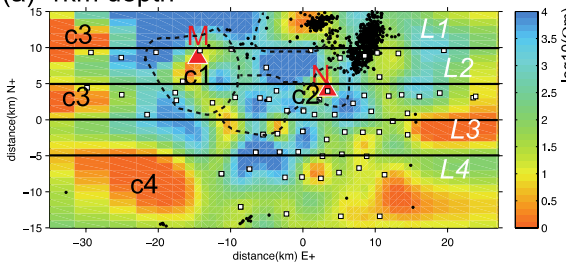

(b) 3km depth

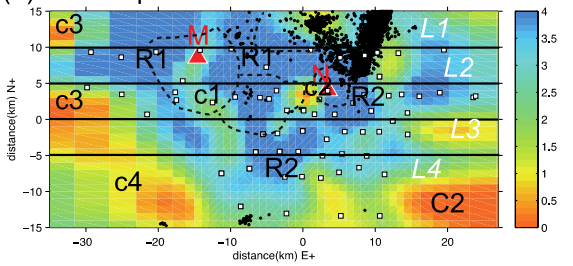

(c) 5km depth

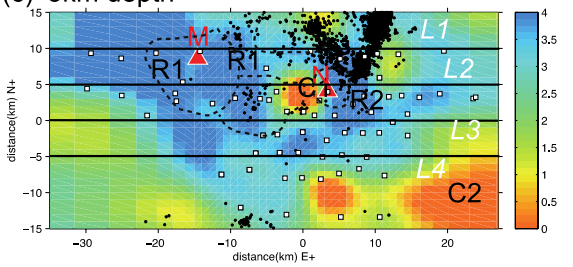

(d) 10km depth

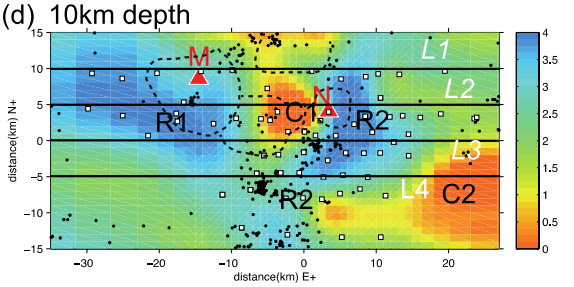

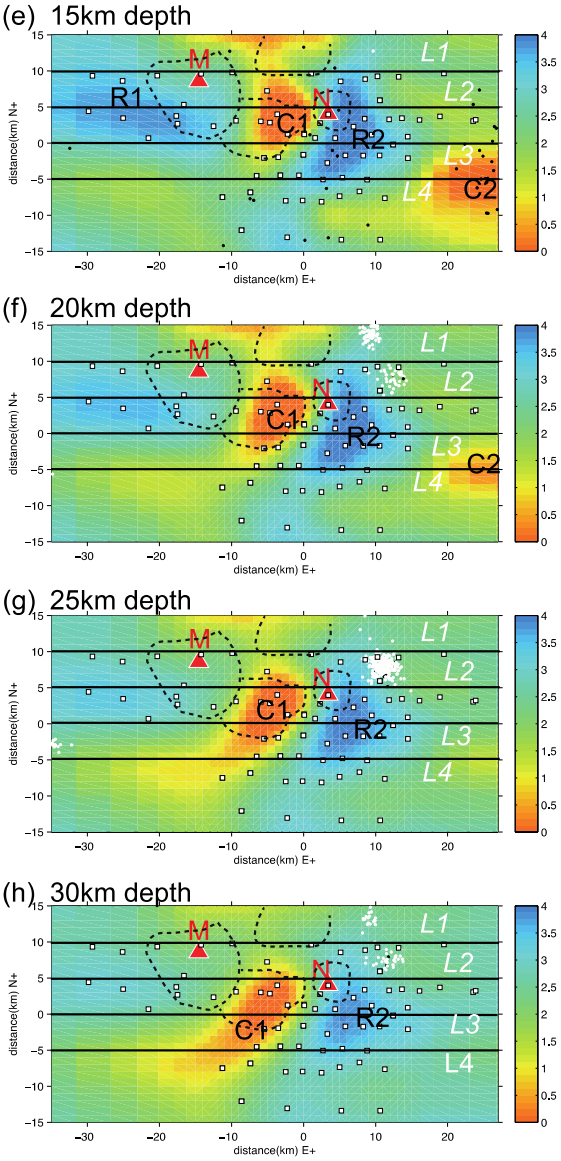

Figure 3: Resistivity depth sections for (a) 1 km, (b) 3 km, (c) 5 km, (d) 10 km, (e) 15 km, (f) 20 km, (g) 25 km, and (h) 30 km (Ogawa et al., 2014). The color denotes log10 (resistivity). The red triangles labeled N and M denote Naruko volcano and Mukaimachi caldera, respectively. The dotted line shows the outlines of the calderas as shown in Figure 1. The black and white dots represent hypocenters of tectonic earthquakes and long-period volcanic earthquakes at respective depths from the 1997 to 2011 JMA catalogue.

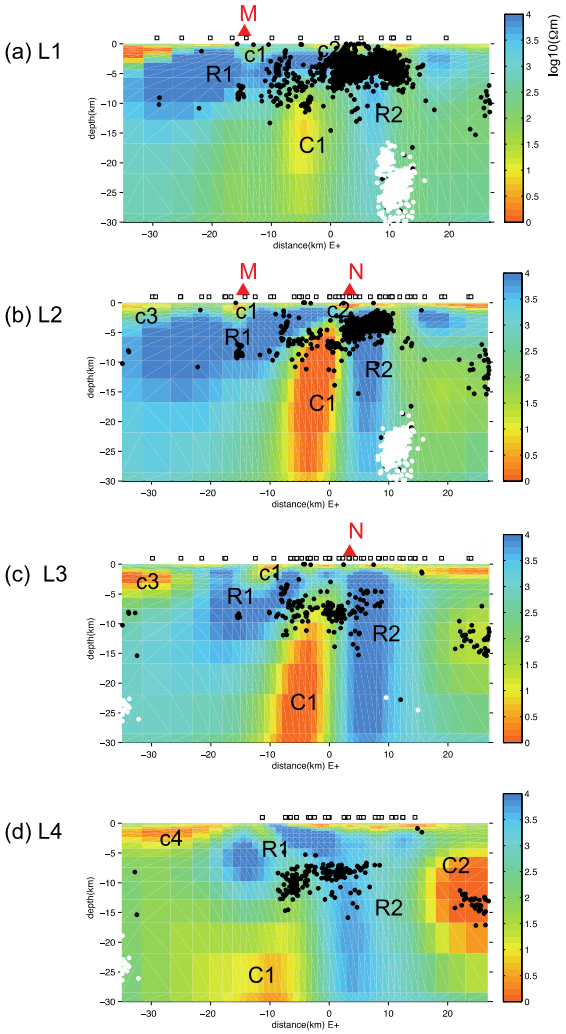

Figure 4: Resistivity sections for profiles L1 (a), L2 (b), L3 (c), and L4 (d) in Figure 1 (Ogawa et al., 2014). The black and white dots indicate tectonic earthquakes and long-period volcanic earthquakes, respectively. The triangles on the surface denote Quaternary volcanoes. M and N indicate the locations of Naruko volcano and Mukaimachi caldera, respectively.

REFERENCES

Asamori K, Umeda K, Ogawa Y, Oikawa T: Electrical resistivity structure and helium isotopes around Naruko volcano, northeastern Japan and its implication for the distribution of crustal magma. *Int J Geophys* 2010, 2010: 1–7. doi:10.1155/2010/738139 (2012)

Asanuma, H., Muraoka, H., Tsuchiya, N., and Ito, H.: The concept of the Japan Beyond-Brittle Project (JBBP) to develop EGS reservoirs in ductile zones, Geothermal Resources Council Transactions, 36, , 359-364. (2012)

Bertrand E, Caldwell T, Hill G, Wallin E, Magnetotelluric imaging of upper-crustal convection plumes beneath the Taupo Volcanic Zone, New Zealand. Geophys Res Lett. doi: 10.1029/2011GL050177 (2012)

Christensen NI: Poisson's ratio and crustal seismology. *J Geophys Res*, 101: 3139. doi:10.1029/95JB03446 (1996)

Dobson P, Asanuma H, Huenges E, Poletto F, Sanjuan B, Dobson P, Asanuma H, Huenges E, Poletto F, Reinsch T. Supercritical Geothermal Systems - A Review of Past Studies and Ongoing Research Activities, *42nd Workshop on Geothermal Reservoir Engineering*. (2017)

Frioleifsson GO, Sigurdsson O, Porbjörnsson D, Karlsdóttir R, Gíslason P, Albertsson A, Elders WA. Preparation for drilling well IDDP-2 at Reykjanes. Geothermics 49:119–126. doi: 10.1016/j.geothermics.2013.05.006 (2014)

Fukino H., Three-dimensional crustal resistivity structure around the Onikobe caldera revealed by magnetotellurics. Master thesis, Tokyo Institute of Technology (2011)

Gasperikova E, Rosenkjaer GK, Arnason K, Newman GA, Lindsey NJ. Resistivity characterization of the Krafla and Hengill geothermal fields through 3D MT inverse modeling. Geothermics 57:246–257. doi: 10.1016/j.geothermics.2015.06.015 (2015)

Hasegawa A, Nakajima J, Umino N, Miura S: Deep structure of the northeastern Japan arc and its implications for crustal deformation and shallow seismic activity. *Tectonophysics*, 403: 59–75. doi:10.1016/j.tecto.2005.03.018 (2005).

Hashin Z, Shtrikman S: On some variational principles in anisotropic and nonhomogeneous elasticity. *J Mech Phys Solids*, 10: 335–342. 10.1016/0022-5096(62)90004-2 (1962)

Hill GJ, Bibby HM, Ogawa Y, Wallin EL, Bennie SL, Caldwell TG, Keys H, Bertrand EA, Heise W, Structure of the Tongariro Volcanic system: Insights from magnetotelluric imaging. Earth Planet Sci Lett. doi: 10.1016/j.epsl.2015.10.003 (2015)

Horiguchi K, Ueki S, Sano Y, Takahata N, Hasegawa A, Igarashi G: Geographical distribution of helium isotope ratios in northeastern Japan. *Island Arc*, 19: 60–70. doi:10.1111/j.1440–1738.2009.00703.x (2010)

Ichiki, M., Y. Ogawa, T. Kaida, T. Koyama, M. Uyeshima, T. Demachi, S. Hirahara, Y. Honkura, W. Kanda, T. Kono, et al. , Electrical image of subduction zone beneath northeastern Japan, *J. Geophys. Res. Solid Earth*, 120, 7937–7965, doi:10.1002/2015JB012028. (2015)

Ingham MR, Bibby HM, Heise W, Jones KA, Cairns P, Dravitzki S, Bennie SL, Caldwell TG, Ogawa Y, A magnetotelluric study of Mount Ruapehu volcano, New Zealand. Geophys J Int. doi: 10.1111/j.1365-246X.2009.04317.x (2009)

Iwamori H: Transportation of H_2O and melting in subduction zones. *Earth Planet Sci Lett*, 160: 65–80. doi:10.1016/S0012–821X(98)00080–6 (1998)

Kawamoto T, Kanzaki M, Mibe K, Matsukage KN, Ono S: Separation of supercritical slab-fluids to form aqueous fluid and melt components in subduction zone magmatism. *Proc Natl Acad Sci USA*, 109: 18695–18700. doi:10.1073/pnas.1207687109 (2012)

Mitsuhata Y, Ogawa Y, Mishina M, Kono T, Yokokura T, Uchida T: Electromagnetic heterogeneity of the seismogenic region of 1962 M6.5 Northern Miyagi Earthquake, northeastern Japan. *Geophys Res Lett*, 28: 4371–4374. 10.1029/2001GL013079 (2001)

Nesbitt BE, Electrical resistivities of crustal fluids. *J Geophys Res*, 98: 4301. doi:10.1029/92JB02576 (1993)

Ogawa Y, Honkura Y, Mid-crustal electrical conductors and their correlations to seismicity and deformation at Itoigawa-Shizuoka Tectonic Line , Central Japan. Earth Planets Space 56:1285–1291. (2004)

Ogawa Y, Ichiki M, Kanda W, Mishina M, Asamori K Three-dimensional magnetotelluric imaging of crustal fluids and seismicity around Naruko volcano, NE Japan. *Earth Planets Space* 66:158. doi: 10.1186/s40623-014-0158-y. (2014)

Ogawa Y, Mishina M, Goto T, Satoh H, Oshiman N, Kasaya T, Takahashi Y, Nishitani T, Sakanaka S, Uyeshima M, Takahashi Y, Honkura Y, Matsushima M: Magnetotelluric imaging of fluids in intraplate earthquake zones, NE Japan back arc. *Geophys Res Lett* 2001, 28: 3741–3744. 10.1029/2001GL013269. (2001)

Okada T, Matsuzawa T, Nakajima J, Uchida N, Yamamoto M, Hori S, Kono T, Nakayama T, Hirahara S, Hasegawa A: Seismic velocity structure in and around the Naruko volcano, NE Japan, and its implications for volcanic and seismic activities. *Earth Planets Space*, 66: 114. doi:10.1186/1880–5981–66–114 (2014)

Pommier A, Le-Trong E: "SIGMELTS": a web portal for electrical conductivity calculations in geosciences. *Comput Geosci*, 37: 1450–1459. doi:10.1016/j.cageo.2011.01.002 (2011)

Saishu H, Okamoto A, Tsuchiya N. The significance of silica precipitation on the formation of the permeable-impermeable boundary within Earth's crust. *Terra Nov* 26:n/a-n/a. doi: 10.1111/ter.12093. (2014)

Shimojuku A, Yoshino T, Yamazaki D: Electrical conductivity of brine-bearing quartzite at 1 GPa: implications for fluid content and salinity of the crust. *Earth Planets Space*, 66: 2. doi:10.1186/1880–5981–66–2 (2014)

Sibson RH, Robert F, Poulsen KH: High-angle reverse faults, fluid-pressure cycling, and mesothermal gold-quartz deposits. *Geology* 1988, 16: 551–555. doi:10.1130/0091–7613 (1988)

Sibson RH: Rupturing in overpressured crust during compressional inversion—the case from NE Honshu, Japan. *Tectonophysics* 2009, 473: 404–416. doi:10.1016/j.tecto.2009.03.016 (2009)

Siripunvaraporn W, Egbert G. WSINV3DMT: Vertical magnetic field transfer function inversion and parallel implementation. Phys Earth Planet Inter 173:317–329. doi: 10.1016/j.pepi.2009.01.013 (2009)

Wannamaker PE, Caldwell TG, Jiracek GR, Maris V, Hill GJ, Ogawa Y, Bibby HM, Bennie SL, Heise H: Fluid and deformation regime of an advancing subduction system at Marlborough, New Zealand. *Nature*, 460: 733–736. doi:10.1038/nature08204 (2009)

Watanabe N, Numakura T, Sakaguchi K, Saishu H, Okamoto A, Ingebritsen SE, Tsuchiya N. Potentially exploitable supercritical geothermal resources in the ductile crust. Nat Geosci 10:140–144. doi: 10.1038/ngeo2879 (2017)

Weatherley DK, Henley RW. Flash vaporization during earthquakes evidenced by gold deposits. Nat Geosci 6:294–298. doi: 10.1038/ngeo1759 (2013)